

# Tunable Lasers Phaselocked to Optical Frequency Comb

Win Indra, Zitong Feng, Meng Ding, Josef Vojtěch and Radan Slavík

**Abstract**— The demand for stable and tunable laser sources is steadily growing across a wide range of applications. Optical Frequency Combs (OFCs) have emerged as a powerful reference standard, offering stable frequency spacing between the comb tones or high optical frequency stability. To obtain low-cost tunable lasers with their carriers or relative frequencies locked, we phaselocked a commercial Telecom grade Integrable-Tunable-Laser-Assembly (ITLA) to an OFC. We demonstrate such phaselock within the telecom C-band (1527 nm - 1565 nm), using sub-mW OFC power corresponding to per-tone power down to nW regime. This enables phaselocking of large number of tunable lasers to the same OFC via passive splitting of the OFC power. We achieved short-term integrated phase noise of 10 mrad and long-term frequency stability measured over 10 hours below  $\pm 0.01$  Hz.

**Index Terms**— phase locked, tunable laser, frequency comb, frequency stability, terahertz source.

## I. INTRODUCTION

Optical frequency combs (OFCs) have revolutionized the field of metrology, where they provide a gearbox between radio frequencies (RF) and optical frequencies. Locking of a stable laser to one of the comb tones of an OFC can be used to generate a high-power, single-frequency signal that can be used in demanding metrology applications, e.g. as an optical frequency reference [1], as well as in diverse fields outside of metrology, e.g., in telecommunications, (where comb-locked laser based transmitters have been shown to enable doubling of reach [2]), and for microwave/terahertz signal generation [3]. In these non-metrological applications, there is often the need to phaselock more than one laser and/or the laser wavelength needs to be tunable. For example, for terahertz signal generation, the spacing between the two lasers needs to be tunable (e.g., by up to 8 nm for 0-1 THz generation). In

telecommunications, wavelength of the signaling lasers is often required to be tunable to allow for flexible allocation of DWDM or flexi-grid channels. These applications are often strongly cost constrained, requiring low-cost OFC, low-cost tunable lasers, minimum and low-cost optical components, and cheap and low-power consuming (i.e., integrated, low-bandwidth) electronics for phase locking.

To address this need, we recently suggested frequency locking of a telecom-grade tunable laser (ITLA laser telecom standard) to an all-fiber, compact, self-starting OFC using a low-speed digital electronics platform (FPGA, on Red Pitaya evaluation board [4]) [5]. Further, we showed how this method can be modified to allow for continuous tuning/control (not limited by the comb tone spacing) of the locked laser across the entire tuning range [5]. Such continuous tuning is difficult to achieve with alternative locking techniques such as optical injection locking [6].

Despite this progress, the presented system required tunable bandpass filters (one for each locked laser) and relatively high power from the OFC tone to which it was locked, requiring optical amplification or high-power OFC. The OFC power requirement and tunable bandpass filters increased the overall cost and complexity. Additionally, tunable lasers usually have limited control bandwidth, which limits the phaselock loop bandwidth. Unfortunately, it contrasts with the need of high phaselock loop bandwidth required for tunable lasers due to their worse stability than non-tunable lasers usually used for phase-locking. Although previous studies [5] showed ability to phase lock despite this trade-off, no systematic study has been carried to investigate limits of performance due to these limitations.

Here, we show a systematic study of ITLA laser locking into an OFC. Firstly, we show that using double- $\text{PI}^2$  (proportional-double-integrator),  $\text{PI}^4$ , phaselock loop filter as opposed to usually-used single  $\text{PI}^2$  enables fivefold increase of the loop bandwidth (reaching the ITLA laser control bandwidth), leading to significantly better performance in terms of phase noise, residual jitter, and frequency error variations. Further, we investigate minimum OFC tone power needed for stable, low-noise phaselock and optimize the detection circuit to enable entire OFC comb to be used without any pre-filtering, eliminating the need for tunable optical filters. This optimization also leads to reduced requirements on the OFC power needed for the phaselock, enabling low OFC powers to be used per locked laser, increasing the number of lasers that can be locked with single OFC by simply passively splitting its power with a single  $1 \times N$  coupler, Fig. 1.

Manuscript received xx xx, xxxx; revised xx xx, xxxx; accepted xx xx, xxxx. Date of publication xx xx, xxxx; date of current version xx xx, xxxx. The data that support the findings of this study are available at the University of Southampton research repository (DOI: [xxx.xxx.xxx](#)).

Win Indra (w.a.indra@soton.ac.uk), Meng Ding and Radan Slavík are with the Optoelectronic Research Centre, University of Southampton, SO17 1BJ, UK.

Zitong Feng is with the Optoelectronic Research Centre, University of Southampton, SO17 1BJ, UK and now with National Physical Laboratory, Teddington, TW11 0LW, UK.

Josef Vojtěch is with CESNET a.l.e Praha 6, 160 00, Czechia.

## II. PRACTICAL CONSIDERATIONS

The envisaged system is sketched in Fig. 1. In this proposed configurations, requirements on the OFC in terms of frequency spacing, flatness (variation in OFC tones powers), and to a certain degree (as we discuss later) also the output power are not critical. We believe that one of good OFC candidates (especially for operation in the telecom C-band) is that presented in [7],[8]. It uses only few passive fiber components spliced together, and a single, 1480-nm telecom-grade, 200-mW pump laser. As the OFC is not subject of our study, we used here an OFC available in our laboratory, which consisted of Menlo FC1500 oscillator, providing 0.5 mW over 77 nm FWHM, comb spacing of 250 MHz, further details are provided later. As we show later, the performance of the earlier-mentioned compact comb should provide a practical alternative.

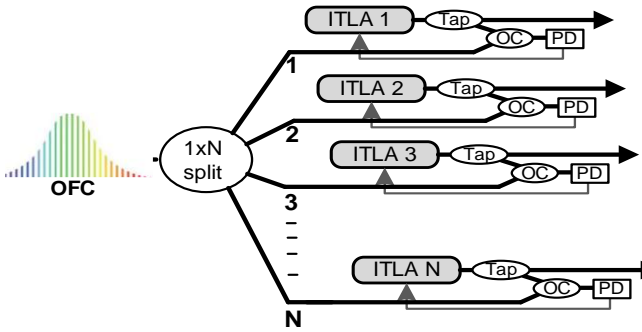


Fig. 1. The envisaged system that comprises minimum optical hardware, low optical powers, and low-speed electronics for ultimate power efficiency. In the example shown here, a low-power (e.g., 10 mW) OFC that emits over the entire C-band (e.g., as shown in [7]) is passively spited by N. N can be, e.g., two for tunable THz synthesis or >10 for a flexigrid telecom transmitter. A set of Integrable Tunable Lasers Assembly (ITLA) lasers are then phase-locked to the desired OFC tones with arbitrary offset (for ultimate tunability), each using one 1xN splitter output and a small tap (e.g., <10%) off the tunable lasers, supplying most of lasers power for the useful output. The phaselock requires very low comb power, e.g., sub-1 mW of the entire OFC (supporting  $N > 10$  with 10-mW OFC) with corresponding per-comb power as low as 1 nW. OC: Optical Coupler, PD: Photodiode.

In terms of ITLA tunable lasers, we use telecom-grade ITLA-packaged lasers with maximum output power of 40 mW for which we set up the wavelength through their software. They also have modulation input to their phase section used for the feedback.

For feedback control, we used FPGA-based board Xilinx Zynq 7010 implemented on Red Pitaya evaluation board that was programmed to enable two parallel  $PI^2$  controllers [4]. Its clock speed was modest at 64 MHz, providing low cost and low power consumption. As we show later, its bandwidth is well-matched to the modulation bandwidth of the used tunable lasers.

Phase locking was performed with 30 MHz offset, however, this could be changed with the used FPGA boards in the range of 10 – 60 MHz. This could be extended to arbitrary number by using additional RF synthesizer and mixer, as we showed in [5].

## III. EXPERIMENTS

In our vision, Fig. 1, OFC is first split passively to serve multiple phase-locked lasers. As such, lower OFC power required for phase locking of each tunable lasers would enable more lasers to be phase locked with the same OFC. In scenarios where only one or very few lasers need to be locked, this would reduce requirements on optical power of the OFC, reducing cost and power consumption. Thus, our first focus was to investigate minimum optical power required to lock our tunable lasers while characterizing the short and long-term performance. Firstly, we locked two identical tunable lasers to each other using set-up shown in Fig. 2, as this configuration provides signal not influenced by beating with multiple comb tones. This sets the benchmark of the best-achievable performance. Subsequently, we verified that similar performance and minimum power levels can be achieved when using OFC as master signal and characterized the performance using set-up schematically shown in Fig. 3.

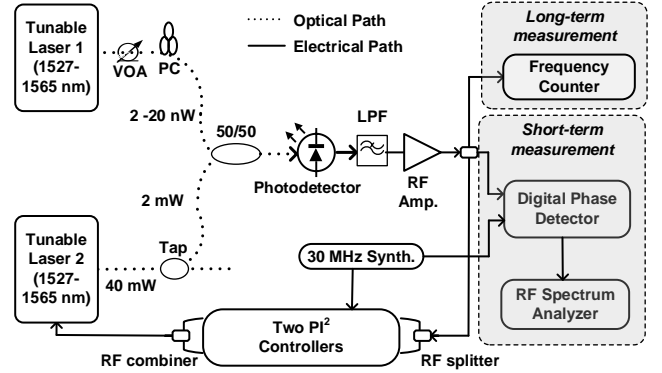


Fig. 2. Schematics of phase locking of two ITLA tunable lasers, one with power of 2 mW (1 mW reaching the photodetector after passing through the 50/50 coupler) and the other with low power, ranging from 1 nW (lowest power at which we achieved stable lock) to 10 nW (2-20 nW prior to the 50/50 coupler). VOA: Variable Optical Attenuator, PC: Polarization Controller, LPF: Low Pass Filter.

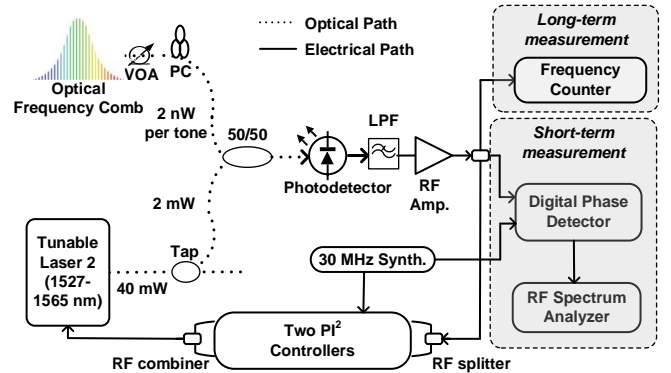


Fig. 3. Schematics of phase locking of ITLA tunable laser to OFC with power set at 2 nW for comb tone used for locking (1 nW reaching the photodetector). VOA: Variable Optical Attenuator, PC: Polarization Controller, LPF: Low Pass Filter.

The used C-band tunable ITLA lasers provided 40 mW output power. Their phase section that controls the laser carrier frequency was used for the feedback. We measured its bandwidth to be 100 kHz. The used OFC (total power: 0.5 mW, comb tone spacing: 250 MHz, 10-dB bandwidth: 77 nm) has its spectrum measured by Optical Spectrum Analyzer (OSA) with resolution of 0.5 nm shown in Fig. 4, where individual tones are not resolved due to their close spacing. Per-tone power was 1.1 nW at 1530 nm, 2.3 nW at 1550 nm, and 3.7 nW at 1565 nm.

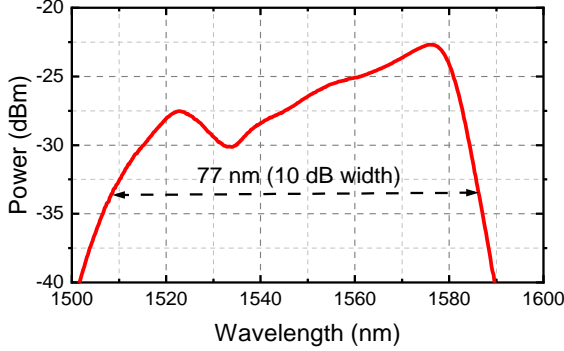


Fig. 4. Spectrum on the used OFC with total power of 0.5 mW and per-comb powers of 1.1 nW at 1530 nm, 2.3 nW at 1550 nm, and 3.7 nW at 1565 nm.

After combining the two signals at 50/50 coupler, the beating signal was detected with an amplified detector (Menlo FPD310), which had bandwidth of 10-1000MHz and maximum input power of 2 mW. As our OFC got power below 1 mW, we decided to keep tunable laser power at the photodetector input fixed at 1 mW, avoiding detector saturation even when using full OFC power for the photodetection, but at the same time, ensuring optimized signal-to-noise ratio, as the total power incident to the photodetector was always above 1 mW (above half of its maximum power). At the same time, 2 mW tapped off the tunable laser (corresponding to 1 mW incident to the photodetector after passing through the 50/50 combiner) is suitably small fraction of the total tunable laser power of 40 mW, ensuring most of the laser power can be used in applications.

The photodetected signal was low-pass filtered with a 50-MHz low-pass filter, isolating the 30-MHz beating of the two lasers (as mentioned earlier, we target locking at 30 MHz offset). This also filters out high-frequency noise and beating of comb tones and of the signal with other comb tones. The beating signal was then amplified using RF amplifier (Mini-Circuits ZFL-500HLN+) and subsequently split in three: for long-term measurement, short-term measurement, and for providing the feedback, Fig. 2 and Fig. 3. The phaselock controller based on Red Pitaya evaluation board had two independent inputs and outputs and we used each of them as a proportional-double-integrator ( $PI^2$ ) controller implemented as described in [4]. The input (beat) signal to the controller had frequency of 30 MHz and peak-to-peak amplitude of  $\pm 0.6$  V. The two Analog to Digital Converters (ADC) had full scale voltage range of  $\pm 1$  V. The digitized beat signal was filtered with a digital bandpass filter with a bandwidth of 3.8 MHz. Its control bandwidth was primarily limited by the delay

associated with the input analog-to-digital and output digital-to-analog conversions delay and was estimated to be 225 kHz [4]. We fed the error signal into both controllers via a passive RF splitter. After parallel processing of the two identical signals with the two independent  $PI^2$  controllers on the Red Pitaya board, we combined both outputs using a passive RF combiner. Combined their output, implementing two double-integrators gain ( $PI^4$ ) controller. In practice, this could be realized using a single input and single output and re-programming the FPGA, which we plan to implement in the future, enabling using one Red Pitaya for locking of two lasers. The feedback bandwidth is expected to be limited mainly by the laser modulation input bandwidth (100 kHz), with all other components having bandwidth  $>200$  kHz.

#### A. Short-term stability measurement

Short-term stability (observation time below 0.1 s, corresponding to  $>10$  Hz) was characterized using digital phase detector and subsequent spectrum analysis of the obtained signal. Digital phase detector has several advantages over often-used frequency mixer. Firstly, it has low cross-sensitivity to amplitude noise. Further, it has larger dynamic range not limited by the periodic  $2\pi$  variation in the response.

As mentioned earlier, we investigated phase locking of two lasers first, as shown in Fig. 2. Subsequently, **Error! Reference source not found.** shows phase noise measured for the lowest power (measured at the photodetector input) for which we could achieve stable phase lock of 1 nW, as well as for slightly higher powers of 5 nW and 10 nW, both for locking two tunable lasers and a tunable laser lock to OFC. Unless stated otherwise, we used  $PI^4$  controller for the feedback.

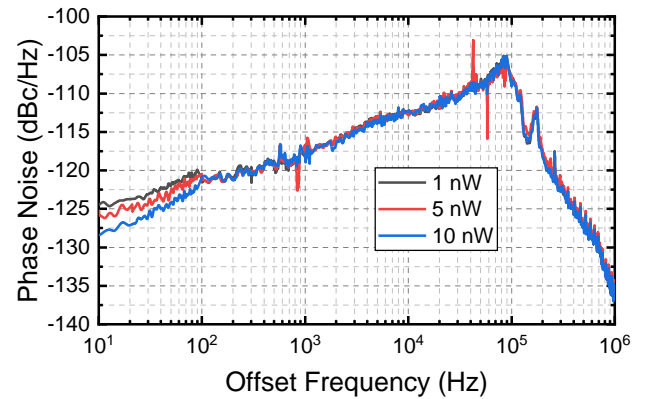


Fig. 5. Phase noise of beat signal between two tunable lasers with powers of 1 mW and 1-10 nW, respectively.

The phase noise above 80 kHz offset frequency corresponds to that of the free-running lasers, as we show later. Below 80 kHz, the feedback produces phase noise that inversely decreases with offset frequency, as expected for well-designed phase locking system. The difference observed when varying laser power (in the range of 1-10 nW) is observed at low frequencies below 100 Hz, reaching few dBs difference at 10 Hz. We believe this small difference comes from

environmentally – related noise, as signal in this low-frequency region kept slightly fluctuating with time. The key conclusion is that 1 nW (-60 dBm) provides sufficient power for phase locking with minimum penalty on the performance.

Subsequently, we exchanged one tunable laser with our OFC, Fig. 3, and performed locking of a tunable laser to the OFC with identical per-tone power as used in the locking of two lasers of 1-10 nW. Unlike previous studies, we used the entire comb signal (77-nm bandwidth) for photodetection, avoiding any tunable optical bandpass filters, reducing the cost considerably while keeping maximum per-tone OFC power for photodetection. The results is shown in Fig. 6. We observe very similar performance to that obtained when locking two lasers, Fig. 5. This demonstrates negligible penalty from the large number of comb tones incident to the photodetector.

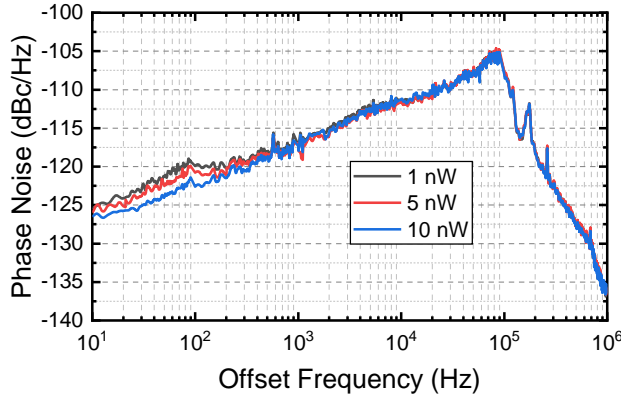


Fig. 6. Phase noise of the beat signal between a tunable laser (power of 1 mW) and OFC with per-tone power of 1-10 nW at the wavelength of 1550 nm.

In the following study, we focus on detailed characterization of our OFC-locked tunable laser set-up (Fig. 3) using 1 nW per-tone OFC power. Fig. 7 shows comparison of phase noise measured on beating of the free running laser with the OFC comb tone and noise obtained when using  $PI^2$  and  $PI^4$  controllers. Their optimum parameters, optimized by observing phase noise while varying them, are summarized in Table 1 and Table 2. Fig. 7 also shows the noise floor measured by connecting the measurement input port of the digital phase detector with a copy of the reference signal.

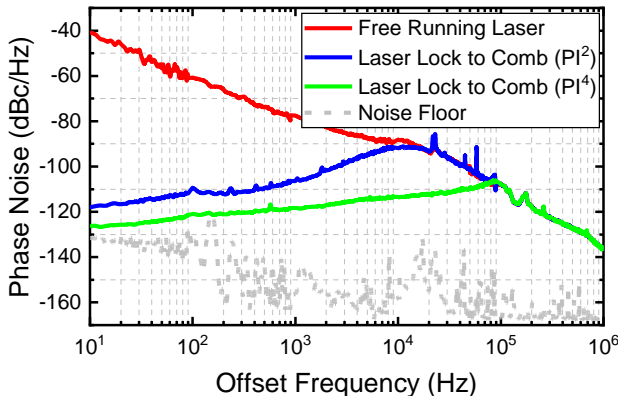


Fig. 7. Phase noise of the beat signal between a tunable laser (power of 1 mW) and OFC with per-tone power of 1 nW at the wavelength of 1550 nm for

free-running laser (blue), when phaselocked using one double-integrator ( $PI^2$ , blue), and using two double-integrators ( $PI^4$ , green). Measurement noise floor is also shown (grey, dashed).

TABLE 1 Optimum parameters for single  $PI^2$ .

Quantity	Value
Proportional gain, $k_p$	7.3
Integrator gain $k_i$	$1.74 \times 10^4$
2 <sup>nd</sup> Integrator gain $k_{ii}$	$1.66 \times 10^3$

TABLE 2 Optimum parameters for two  $PI^2$  ( $PI^4$ )

Quantity	First $PI^2$	Second $PI^2$
Proportional gain, $k_p$	2.6	12.5
Integrator gain, $k_i$	$1.2 \times 10^6$	$1.38 \times 10^3$
2 <sup>nd</sup> Integrator gain $k_{ii}$	$3.02 \times 10^2$	$2.34 \times 10^4$

The result shows that  $PI^4$  enabled us to achieve higher control bandwidth (from 20 kHz to 100 kHz) and better noise suppression at low offset frequencies than with the  $PI^2$  controller. Further,  $PI^4$  gives reductions of 13 and 20 dB in phase noise at 1 and 10 kHz from the carrier frequency, respectively, as compared to  $PI^2$ . The  $PI^2$  and  $PI^4$  suppress the phase noise by 78 dB to 87 dB at 10 Hz offset frequency as compared to the free running laser. The phase noise at 10 Hz obtained with the  $PI^4$  is approaching that of our measurement noise floor, Fig. 7.

Further, we investigated how the performance depends on the wavelength. Fig.8 shows phase noise measured across the C-band, specifically at 1530, 1550, and 1565 nm. Here, we see that the performance is similar at all wavelengths, including 1530 nm, where the relevant comb tone has power smaller than comb tones at other wavelengths (e.g., over 6 dB weaker than at 1575 nm, Fig. 4), showing robustness of this technique to non-uniformity in the OFC power across its spectrum.

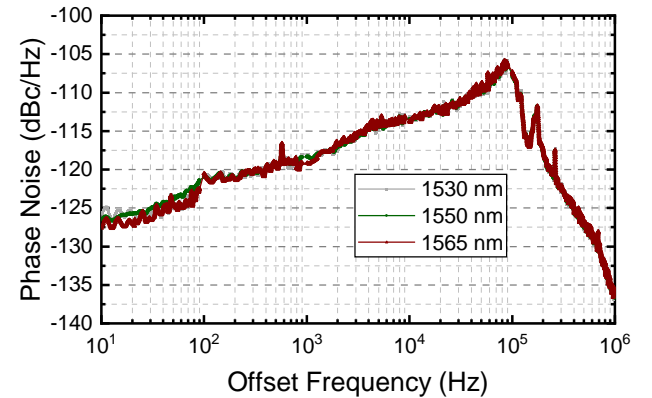


Fig. 8. Phase Noise of beat signal of locking tunable laser to the OFC at different wavelengths with relevant OFC power set to 1 nW.

Finally, we calculated phase noise jitter by integrating the



phase noise measured with the  $PI^2$  and  $PI^4$  controllers, Fig. 9. When integrating over the entire measurement bandwidth (10 Hz – 1 MHz), we have obtained 35 mrad for  $PI^2$  and 10 mrad for  $PI^4$ , respectively. Given the limited bandwidth and low-cost electronics used, this represents good performance, e.g. jitter more than 100 times lower than reported in [9].

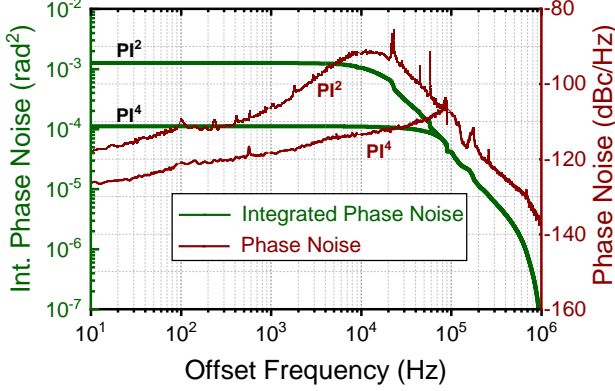


Fig. 9. Phase noise jitter calculated from the measured phase noise of OFC-locked tunable laser (with per-tone power of 1 nW) when locked using  $PI^2$  and  $PI^4$  feedback controller.

### B. Long-term stability

Long-term stability (observation times over 100  $\mu$ s or 1 s, corresponding to frequencies below 10 kHz and 1 Hz, respectively) were measured using a frequency counter (Keysight 53230A).

Firstly, we measured frequency error over time when setting sampling time at 1 s. We performed this measurement over 10 hours to show robust and stable locking. The result is shown in Fig. 10. for both,  $PI^2$  and  $PI^4$  control. The peak-to-peak frequency error stayed within  $\pm 0.01$  Hz for  $PI^4$ , which is about five times better than obtained with the  $PI^2$ , showing that the benefit of  $PI^4$  is significant even over long observation times. The achieved performance is good, e.g., 100 times lower frequency variation (with  $PI^4$ ) when compared to the results shown in the literature, e.g., in [10].

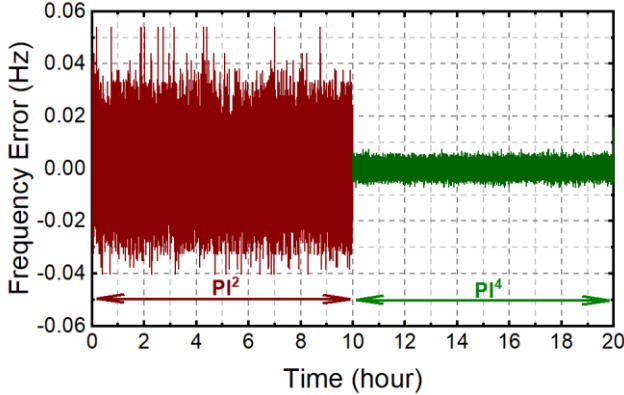


Fig. 10. Frequency error of OFC-laser beat signal with one double-integrator ( $PI^2$ ) and two double-integrators ( $PI^4$ ) using 1 s gate time, measured over 10 hours.

Further, we calculated Allan deviation from the data show in Fig. 10 and complemented them with data measured at shorter gating time (4  $\mu$ s) to obtain Alan Deviation data over averaging times of 100  $\mu$ s to 1000 s, Fig. 71. Between 100  $\mu$ s and 100 ms, Allan deviation has slope of  $\tau^{-1}$ . For longer observation times, the slope is reduced, likely due to low-frequency drift in our setup. Importantly,  $PI^4$  result is for all averaging times about one order of magnitude better than that obtained with the  $PI^2$ . At 1 s averaging time, the stability with  $PI^4$  is  $2 \times 10^{-14}$ .

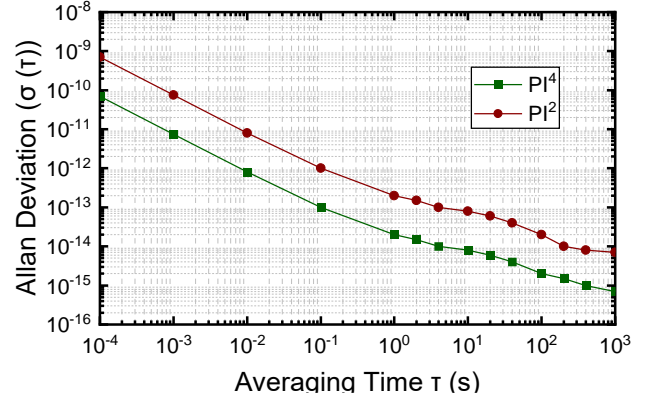


Fig. 7. Allan deviation calculated from the frequency counter data when a tunable laser is locked to the OFC using two double-integrators ( $PI^4$ ) and one double-integrator ( $PI^2$ ), normalized to the laser carrier frequency (192 THz).

### C. Discussion

In our work, we focused on performance characterization of a single tunable laser locked to the OFC. In practice, more lasers could be locked to the same OFC by passively splitting it, as outlined in our vision, Fig. 1. Locking two lasers to different parts of the OFC spectrum with subsequent photomixing [11] can be used to generate RF signals, up to 4.5 THz when considering the used C-band tunable lasers or up to 9 THz when combining one C-band and one L-band tunable lasers. The key advantage of OFC-locking is the strongly-reduced phase noise of the generated beat signal as compared to beat produced by two independent lasers. Let us estimate performance achievable in such configuration. Each laser is locked to the respective comb tone and the fractional frequency stability of this locking can be calculated by re-normalizing data shown in Fig. 7 to the frequency spacing between the two lasers and multiplying by  $\sqrt{2}$  to account for two lasers. The result for averaging time of 1 s and different laser spacing is shown in

Fig. 8. As expected, the fractional frequency instability is improving with frequency spacing between the lasers, as the locking stability remains constant, but the frequency difference increases. We also plot fractional frequency instability of our OFC limited by its RF reference (Timetech 5.10) of  $5 \times 10^{-13}$  at averaging time of 1 s. We can conclude we are not limited by the stability of our OFC, as the stability of the two laser beating is lower than that of our OFC. However, OFC with lower-quality RF reference (e.g., with instability in the  $10^{-11}$  level at 1 s) would result in the beating being limited by the OFC rather than our locking. As this is level of RF reference found in typical crystal oscillators (as compared to our

laboratory-grade high-quality RF reference), it is expected that the OFC performance will be typically the limiting factor, with our laser phase locking providing smaller contribution to the overall stability, showing more than sufficient level of phase locking performance.

For comparison, we also show fractional frequency instability from other sources (adapted from [13]) in

Fig. 82. Better results are obtained with high-quality OFCs [13], however, comparing to photomixing two CW lasers [14], [15] [16], our technique shows up to 2 orders of magnitude better fractional frequency instability for frequencies above 0.1 THz. It also gives comparable result to photomixing using a microcomb [17], [18] or a quantum cascade laser [19], [20], [21]. Both these techniques, however, lack tunability provided by our technique.

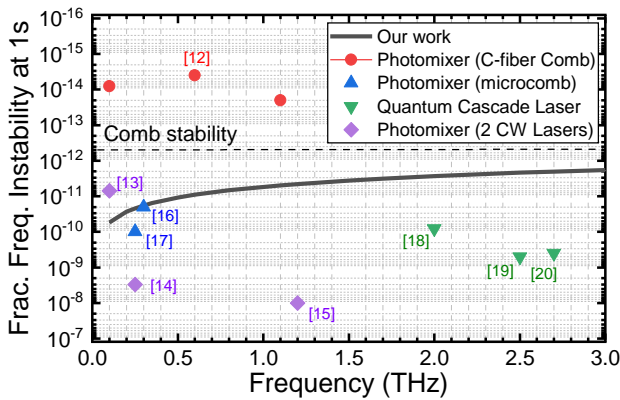


Fig. 82. Fractional frequency instability of the beat signal at 1 s averaging times for various beat frequencies expected from our system and its comparison with the state-of-the art terahertz sources (adopted from [13]).

Given the small OFC tone spacing in our demonstration (250 MHz), it is important to consider how we could ensure that we pick the right OFC tone to lock to, as tunable lasers may not provide such fine calibration via their internal etalon. One option would be to use a comb with slightly higher spacing, e.g., few GHz in combination with beat note tuning shown in [5]. Another possibility would be using an etalon with free-spectral range smaller than that used in ITLA lasers to provide fine resolution of the laser wavelength.

As for the  $PI^4$  controller, we implemented it via splitting the input signal and then feeding two independent  $PI^2$  controllers in parallel, combining their signal at the output. This proved suitable for our proof-of-concept experiment, especially given there are already two independent controllers at the Red Pitaya board. However, a more practical implementation would be re-programming the FPGA board to implement directly the  $PI^4$  controller using single-input and single-output (enabling locking of two independent lasers with the same Red Pitaya board). This should be reasonably straightforward with appropriate FPGA programming skills.

#### IV. CONCLUSION

We present a practical tunable comb-locked laser system that uses minimum optical hardware and telecom-grade components including tunable lasers and low-bandwidth electronics. It could be combined with a wide range of OFC generators, as it does not have any particular requirements on the OFC spectral flatness or tone spacing.

The relatively low stability of tunable telecom lasers (as compared to laboratory-grade single-frequency lasers) in combination with limited bandwidth of the feedback electronics is managed through design of the phaselocking feedback. We show the benefit of employing two double-integrators and proportional gain ( $PI^4$ ) as compared to routinely-used single double-integrator proportional control ( $PI^2$ ). In particular, the peak-to-peak frequency error measured over 10 hours was reduced five times (to  $\pm 0.01$  Hz) and Allan deviation at 1 s integration time achieved  $2 \times 10^{-14}$ . For shorter observation times, phase noise improved by 10-25 dB over the 10 Hz – 50 kHz frequency range with fivefold increase in the loop bandwidth.

The developed system will be of interest to tunable THz waves generation or for realization of comb-locked transmitters for DWDM systems.

#### ACKNOWLEDGMENT

This work has received support from the EPSRC projects EP/P030181/1 and EP/W037440/1. Win Indra would like to acknowledge support from Indonesian Endowment Fund for Education (LPDP) No. 20201022305177.

#### DATA AVAILABILITY

Data underlying the results presented in this paper will be available at the University of Southampton research repository (DOI: [xxx.xxx.xxx](#)).

#### DISCLOSURES

The authors declare no conflicts of interest.

#### REFERENCES

- [1] T. Fortier and E. Baumann, “20 years of developments in optical frequency comb technology and applications,” *Commun Phys*, vol. 2, no. 1, p. 153, Dec. 2019, doi: 10.1038/s42005-019-0249-y.
- [2] E. Temprana *et al.*, “Overcoming Kerr-induced capacity limit in optical fiber transmission,” *Science* (1979), vol. 348, no. 6242, pp. 1445–1448, Jun. 2015, doi: 10.1126/science.aab1781.
- [3] A. Fokin *et al.*, “High-power sub-terahertz source with a record frequency stability at up to 1 Hz,” *Sci Rep*, vol. 8, no. 1, p. 4317, Mar. 2018, doi: 10.1038/s41598-018-22772-1.
- [4] A. Tourigny-Plante, V. Michaud-Belleau, N. Bourbeau-Hébert, H. Bergeron, J. Genest, and J.-D. Deschênes, “An open and flexible digital phase-locked loop for optical metrology,” *Review of Scientific*

- Instruments*, vol. 89, no. 9, Sep. 2018, doi: 10.1063/1.5039344.
- [5] Z. Feng, A. Tourigny-Plante, J. Vojtěch, J. Genest, D. J. Richardson, and R. Slavík, "Comb-locked telecom-grade tunable laser using a low-cost FPGA-based lockbox," in *Conference on Lasers and Electro-Optics*, Washington, D.C.: Optica Publishing Group, 2021, p. STu1J.4. doi: 10.1364/CLEO\_SI.2021.STu1J.4.
  - [6] Z. Liu and R. Slavík, "Optical Injection Locking: From Principle to Applications," *Journal of Lightwave Technology*, vol. 38, no. 1, pp. 43–59, Jan. 2020, doi: 10.1109/JLT.2019.2945718.
  - [7] R. Slavík, J. Vojtěch, Meng Ding, and D. J. Richardson, "Compact and low-power comb-locked transmitter based on ITLA tuneable lasers," in *45th European Conference on Optical Communication (ECOC 2019)*, Institution of Engineering and Technology, 2019, pp. 189 (3 pp.)–189 (3 pp.). doi: 10.1049/cp.2019.0923.
  - [8] L. C. Sinclair et al., "A compact optically coherent fiber frequency comb," *Review of Scientific Instruments*, vol. 86, no. 8, Aug. 2015, doi: 10.1063/1.4928163.
  - [9] M. Matusko et al., "Fully digital platform for local ultra-stable optical frequency distribution," *Review of Scientific Instruments*, vol. 94, no. 3, Mar. 2023, doi: 10.1063/5.0138599.
  - [10] K. Balakier, L. Ponnampalam, M. J. Fice, C. C. Renaud, and A. J. Seeds, "Integrated Semiconductor Laser Optical Phase Lock Loops," *IEEE Journal of Selected Topics in Quantum Electronics*, vol. 24, no. 1, pp. 1–12, Jan. 2018, doi: 10.1109/JSTQE.2017.2711581.
  - [11] F. Wang et al., "Simple, low-cost, and well-performing optical phase-locked loop for frequency and phase locking of semiconductor lasers," *Appl Opt*, vol. 62, no. 27, p. 7169, Sep. 2023, doi: 10.1364/AO.496663.
  - [12] S.-H. Yang and M. Jarrahi, "Navigating Terahertz Spectrum via Photomixing," *Opt Photonics News*, vol. 31, no. 7, p. 36, Jul. 2020, doi: 10.1364/OPN.31.7.000036.
  - [13] D.-C. Shin, B. S. Kim, H. Jang, Y.-J. Kim, and S.-W. Kim, "Photonic comb-rooted synthesis of ultra-stable terahertz frequencies," *Nat Commun*, vol. 14, no. 1, p. 790, Feb. 2023, doi: 10.1038/s41467-023-36507-y.
  - [14] A. R. Criado et al., "Continuous-Wave Sub-THz Photonic Generation With Ultra-Narrow Linewidth, Ultra-High Resolution, Full Frequency Range Coverage and High Long-Term Frequency Stability," *IEEE Trans Terahertz Sci Technol*, vol. 3, no. 4, pp. 461–471, Jul. 2013, doi: 10.1109/TTHZ.2013.2260374.
  - [15] R. J. Steed et al., "Hybrid Integrated Optical Phase-Lock Loops for Photonic Terahertz Sources," *IEEE Journal of Selected Topics in Quantum Electronics*, vol. 17, no. 1, pp. 210–217, Jan. 2011, doi: 10.1109/JSTQE.2010.2049003.
  - [16] G. Mouret et al., "THz photomixing synthesizer based on a fiber frequency comb," *Opt Express*, vol. 17, no. 24, p. 22031, Nov. 2009, doi: 10.1364/OE.17.022031.
  - [17] T. Tetsumoto, F. Ayano, M. Yeo, J. Webber, T. Nagatsuma, and A. Rolland, "300 GHz wave generation based on a Kerr microresonator frequency comb stabilized to a low noise microwave reference," *Opt Lett*, vol. 45, no. 16, p. 4377, Aug. 2020, doi: 10.1364/OL.398345.
  - [18] T. Tetsumoto, T. Nagatsuma, M. E. Fermann, G. Navickaite, M. Geiselmann, and A. Rolland, "Optically referenced 300 GHz millimetre-wave oscillator," *Nat Photonics*, vol. 15, no. 7, pp. 516–522, Jul. 2021, doi: 10.1038/s41566-021-00790-2.
  - [19] J. R. Freeman et al., "Injection locking of a terahertz quantum cascade laser to a telecommunications wavelength frequency comb," *Optica*, vol. 4, no. 9, p. 1059, Sep. 2017, doi: 10.1364/OPTICA.4.001059.
  - [20] M. Ravaro et al., "Phase-locking of a 25 THz quantum cascade laser to a frequency comb using a GaAs photomixer," *Opt Lett*, vol. 36, no. 20, p. 3969, Oct. 2011, doi: 10.1364/OL.36.003969.
  - [21] S. Barbieri et al., "Phase-locking of a 2.7-THz quantum cascade laser to a mode-locked erbium-doped fibre laser," *Nat Photonics*, vol. 4, no. 9, pp. 636–640, Sep. 2010, doi: 10.1038/nphoton.2010.125.